Transactions of the Materials Research Society of Japan 30[1] 93-96 (2005)

Control of Shape and In-plane Orientation of Self-Assembled $PbTiO_3$ Nanoislands Prepared by MOCVD

Hajime Nonomura, Masaki Nagata[1], Hironori Fujisawa[1], Masaru Shimizu[1], Hirohiko Niu[1] and Koichiro Honda[2]
Himeji Inst. of Tech. /[1]Univ. of Hyogo, 2167 Shosha, Himeji, Hyogo 671-2201
Fax: 81-792-67-4855, e-mail: nonomura.hajime@elnics.eng.himeji-tech.ac.jp
[2]Fujitsu Lab. Ltd., 10-1 Morinosato Wakamiya, Atsugi, Kanagawa 243-0197

Self-assembled $PbTiO_3$ nanoislands were prepared on $Pt/SrTiO_3$ substrates by metalorganic chemical vapor deposition. Pyramidal-shaped (width 17-200 nm, height 5-50 nm), triangular-prism-shaped (width 10-350 nm, length 25-830 nm, height 9-120 nm) and square-shaped (width 40-130 nm, height 4-10 nm) nanoislands with ordered in-plane orientation were formed on $Pt/SrTiO_3$(111), (101) and (001), respectively. These islands were epitaxially grown on the $Pt/SrTiO_3$ substrates and consisted of {100} and {001} facets irrespective of the orientation of the substrates. Piezoresponse force microscopy indicated that the three different types of self-assembled $PbTiO_3$ nanoislands were ferroelectric.
Key words: $PbTiO_3$, self-assembly, nanoislands, ferroelectricity, MOCVD

1. INTRODUCTION

Ferroelectric nanostructures have attracted much interest not only from the viewpoint of high integration of electronic devices, such as non-volatile ferroelectric random access memories (NV-FeRAMs) and nano-actuators in nanoelectromechanical systems (NEMS), but also from that of the finite size effects.

Ferroelectric nanostructures have been fabricated by patterning continuous films using micro processing techniques, such as electron beam (EB) lithography,[1] focused ion beam (FIB) milling,[2,3] EB-induced patterning,[4,5] and imprint lithography.[6] These techniques have a capability of producing well-ordered nanostructures with the desired size and shape. However, the minimum feature size was limited to 70-100 nm, and ferroelectric properties may be degraded by processing damages.[7]

On the other hand, self-assembled process was one of another techniques for the preparation of ferroelectric nanostructures, which have the potential to produce high quality nanostructures smaller than 50 nm without processing damages.[8-15] For example, ferroelectric nanostructures with lateral dimensions 20-50 nm were obtained by chemical solution deposition (CSD),[8,9] sputtering[10] and metalorganic chemical vapor deposition (MOCVD)[11-15] methods. In our previous study, we also fabricated $PbTiO_3$ and $Pb(Zr,Ti)O_3$ nanosized islands on $Pt/SiO_2/Si$ and $Pt/SrTiO_3$ by MOCVD in the Volmer-Weber (V-W) growth mode at the initial stage of thin film growth.[11-15] However, there have been very few reports on structural control of the size, shape and in-plane direction of ferroelectric nanostructure by self-assembled process.[12,14,15]

In this study, we demonstrate control of shape and in-plane orientation of self-assembled $PbTiO_3$ nanoislands epitaxially grown on $Pt/SrTiO_3$(001), (101), (111) substrates by MOCVD. The piezo- and ferroelectric properties of self-assembled $PbTiO_3$ nanoislands are also discussed.

2. EXPERIMENTAL PROCEDURES

For the three-dimensional island growth of $PbTiO_3$, 90 nm-thick Pt thin films were deposited on $SrTiO_3$(111), (101) and (001) single crystals at 630°C by rf magnetron sputtering. Epitaxial growth of Pt thin films on $SrTiO_3$(111), (101) and (001) substrates were examined by XRD pole figure measurements. $PbTiO_3$ self-assembled islands were grown on the $Pt(111)/SrTiO_3(111)$, $Pt(101)/SrTiO_3(101)$ and $Pt(001)/SrTiO_3(001)$ at 540°C by MOCVD using triethyl-*n*-pentoxy lead ($((C_2H_5)_3PbOCH_2C(CH_3)_3$) and tetra-*i*-propoxy titanium ($Ti(O\text{-}i\text{-}C_3H_7)_4$) as precursors, and O_2 as an oxidizing gas. The size of $PbTiO_3$ islands were controlled by changing the deposition time from 5 s to 10 min. The in-plane orientation and epitaxial growth of $PbTiO_3$ islands were examined by XRD pole figure measurements. The size, shape and microstructure of the $PbTiO_3$ islands were observed by atomic force microscopy (AFM) (Seiko Instr. Inc.: SPI-3800N) and transmission electron microscopy (TEM) (JEOL: JEM2010FEG). Piezoelectric and ferroelectric properties of $PbTiO_3$ islands were measured by piezoresponse force microscopy (PFM).

3. RESULTS AND DISCUSSION

From XRD profiles of self-assembled $PbTiO_3$

nanoislands grown for 2-5 min on the $Pt/SrTiO_3(111)$, (101) and (001) substrates, it was found that $PbTiO_3$ nanoislands had (111)-, (101)- and (001)-orientation, respectively. XRD pole figures of the (200), (200) and (220) peaks of $PbTiO_3$, Pt and $SrTiO_3$ for $PbTiO_3/Pt/SrTiO_3(111)$, (101) and (001) revealed the epitaxial growth of $PbTiO_3$ nanoislands on $Pt/SrTiO_3$ substrates.

Figure 1 shows AFM images of self-assembled $PbTiO_3$ nanoislands grown for 10-60 s on $Pt/SrTiO_3(111)$ substrates. When deposition time increased from 10 s to 60 s, lateral size and height of pyramidal shaped islands increased from 35 to 96 nm and 7 to 27 nm, respectively. The in-plane direction of $PbTiO_3$ islands were arranged in an orderly manner because of their epitaxial growth on $Pt/SrTiO_3$. The direction of the apexes of the triangle were arranged along the [112]-direction of $SrTiO_3$ (Fig. 1(a)). Line profiles along A-B and C-D in Fig. 1(c) show that the cross sections of $PbTiO_3$ islands on $Pt/SrTiO_3(111)$ were triangle, which indicates that $PbTiO_3$ islands on $Pt/SrTiO_3(111)$ were triangular-pyramidal shape. Their three side facets were tilted by 50-55° to the Pt(111) surface, which is almost the same as the angle between the {100} and {111} planes, 53.9°, or that between the {001} and {111} planes, 56.4°, calculated from the lattice constants of bulk $PbTiO_3$. Therefore, the three facet planes of the triangular-pyramid were found to be {100} and {001} planes.

Similar growth behavior was observed for $PbTiO_3$ grown for 10-60 s on $Pt/SrTiO_3(101)$, as shown in Fig. 2. When a deposition time was 10 s, square-shaped islands were observed. Average width, length and height of $PbTiO_3$ islands deposited for 10 s were 80, 70 and 10 nm, respectively. As the deposition time was longer than 30 s, average length increased to 250 nm and the shape changed to a rod-shape. The in-plane directions of $PbTiO_3$ islands were arranged along the <010> direction of $SrTiO_3$ due to the epitaxial growth. From line profiles along A-B and C-D in Fig.2(c), the cross-sections along the $<10\bar{1}>$ (A-B) and <010> (C-D) directions were triangle and rectangle, respectively. This result showed that $PbTiO_3$ islands on $Pt/SrTiO_3(101)$ had triangular-prism shape. The

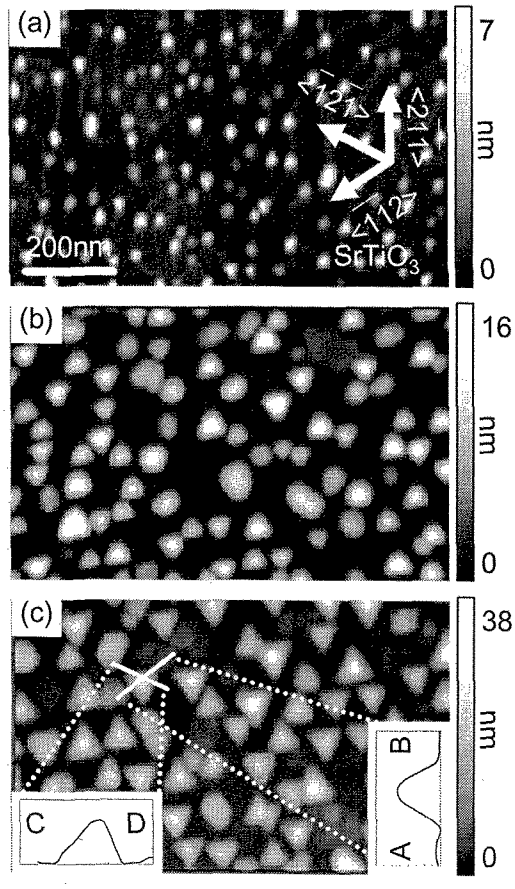

Fig.1 AFM images of self-assembled $PbTiO_3$ islands prepared on $Pt/SrTiO_3(111)$ for (a) 10 s, (b) 30 s and (c) 60 s.

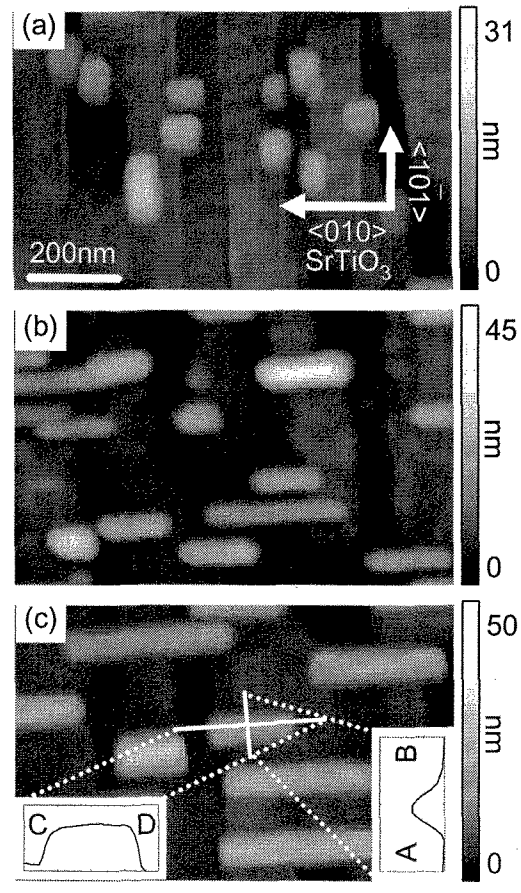

Fig.2 AFM images of self-assembled $PbTiO_3$ islands prepared on $Pt/SrTiO_3(101)$ for (a) 10 s, (b) 30 s and (c) 60 s.

side facets of the triangle (A-B cross-section) and rectangle (C-D cross-section) were tilted by ~45° and ~90° from the Pt(101) surface, respectively, showing that the facets were {100} and {001} planes.

Figure 3 shows dependences of width, length and height of (101)-$PbTiO_3$ islands on the deposition time. When the deposition time increased from 10 s to 10 min, width and height linearly increased from 80 to 280 nm and 10 to 100 nm, respectively. Growth rates along the direction of width (<10$\bar{1}$> direction) and height (<101> direction), which were obtained from the slope of fitted lines, were 19 and 9 nm/min, respectively. On the other hand, the growth rate along the direction of length (<010> direction) decreased from 200 to 34 nm/min at the deposition time of 1 min. This decrease in the growth rate along <010> direction is due to the coalescence of $PbTiO_3$ islands.

From these results, the shape transition in growth of $PbTiO_3$ nanoislands on Pt/$SrTiO_3$(101) is explained by the surface energy for $PbTiO_3$ islands with a square-shape and by the stress relaxation for those with a triangular-prism-shape. At the early growth stage of islands, square shape was favored because the surface energy of the square-shaped islands was smaller than that of triangular-prism-shaped islands for same volume. As the volume of islands increased, island elongated along <010>-direction and minimized the island energy because the elastic relaxation which occurred at the edge of islands lowered the total energy of islands at the growth temperature. This shape transition in growth of strained islands agrees with the theoretical model predicted by J.Tersoff *et al.*[16]

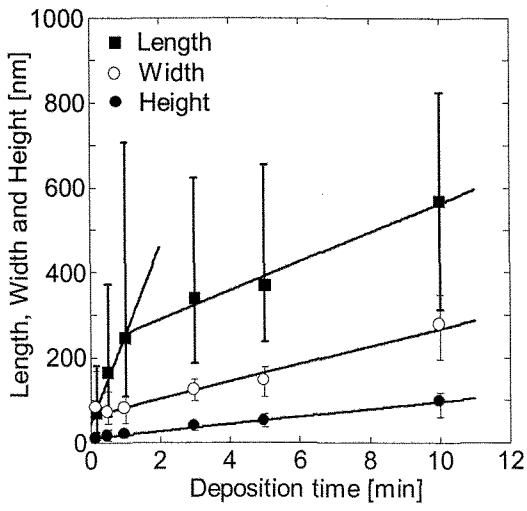

Fig.3 Dependence of width, length and height of $PbTiO_3$ islands on the deposition times. Larger scattering in the length is due to the higher growth rate along <101> direction than those along <101> and <10$\bar{1}$> directions.

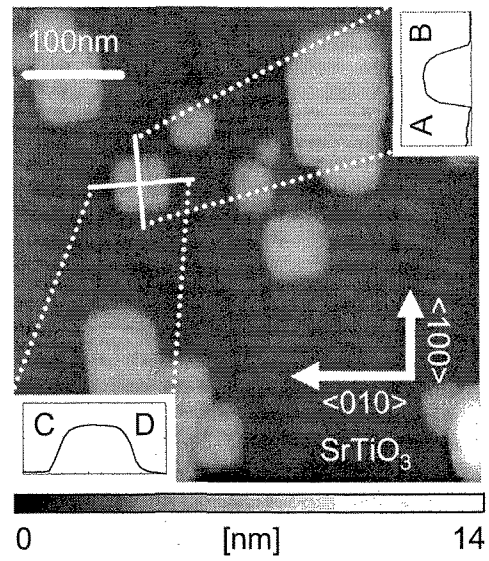

Fig. 4 An AFM image of self-assembled $PbTiO_3$ islands prepared on Pt/$SrTiO_3$(001) for 60 s.

When $PbTiO_3$ was deposited for 60 s on Pt/$SrTiO_3$(001) substrate, square-shaped islands with widths of 30-150 nm and heights of 4-10 nm were observed, as shown in Fig. 4. In-plane orientations of the four sides of the square shape of $PbTiO_3$ islands were <100> and <010>, which corresponded to <100> and <010> directions of $SrTiO_3$. From the line profile along A-B, the edge facets of the square-shaped $PbTiO_3$ islands were normal to the Pt(001) surface and the cross-sectional shape was rectangle. Therefore, the edge facets of the $PbTiO_3$ nanoislands on Pt/$SrTiO_3$(001) were {100} planes, which is the same as that of $PbTiO_3$ nanoislands on Pt/$SrTiO_3$(111) and (101). From these results, it was found that the shape of self-assembled $PbTiO_3$ nano-islands was dependent on the orientation of Pt/$SrTiO_3$ substrates because the islands consisted of {100} and {001} facets regardless of the different orientations of the substrates.

In the next stage, piezoelectric hysteresis loops of $PbTiO_3$ nanoislands were measured by PFM. Figure 5 shows typical piezoelectric hysteresis loop of $PbTiO_3$ nanoislands on Pt/$SrTiO_3$(111). Triangular-prism shaped and square-shaped $PbTiO_3$ nanoislands on Pt/$SrTiO_3$(101) and (001) also showed piezo-response hysteresis loops. These piezoresponse measurements revealed that the three different types of self-assembled $PbTiO_3$ nanoislands were ferroelectric.

In summary, three types (pyramidal-shape, triangular-prism-shape and square-shape) of self-assembled $PbTiO_3$ nanoislands with ordered in-plane direction were obtained on Pt/$SrTiO_3$(111), (101) and (001) substrates by MOCVD. These $PbTiO_3$ nanoislands were

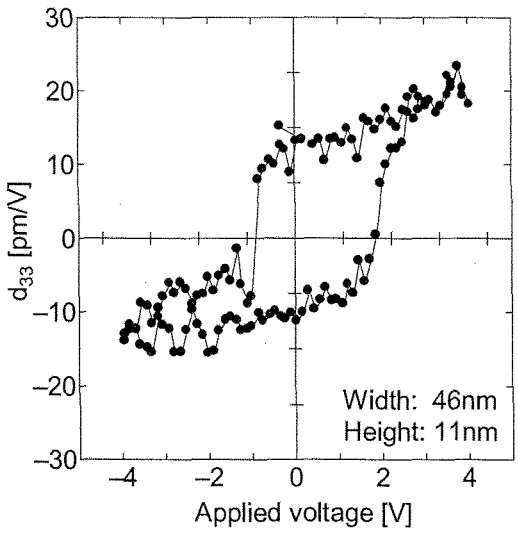

Fig.5 A typical piezoelectric hysteresis loop of $PbTiO_3$ islands on $Pt/SrTiO_3(111)$ grown for 30 s.

epitaxially grown on $Pt/SrTiO_3$ substrates and consisted of {100} and {001} facets irrespective of the orientations of the substrates. Therefore, shape and in-plane orientation of $PbTiO_3$ nanoislands were controlled by introducing of epitaxial relation. Piezoresponse measurements indicated that the three different types of self-assembled $PbTiO_3$ nanoislands had ferroelectricity.

This work was partly supported by a Grant-in-Aid for Scientific Research (B)(2)(12134207) from the Ministry of Education, Culture, Sports, Science and Technology and Research Grants from University of Hyogo and Himeji Institute of Technology.

4. REFERENCES

1 S. Bühlmann, B. Dwir, J. Baborowski and P. Muralt, Appl. Phys. Lett. 80, 3195 (2002).
2 C. S. Ganpule, A. Stanishevsky, Q. Su, S. Aggarwal, J. Melngailis, E. Williams and R. Ramesh, Appl. Phys. Lett. 75, 409 (1999).
3 V. Nagarajan, A. Roytburd, A. Stanishevsky, S. Prasertchoung, T. Zhao, L. Chen, J. Melngailis, O. Auciello and R. Ramesh, Nature Materials 2, 43 (2003).
4 S. Okamura, Y. Yagi, S. Ando, T. Tsukamoto and K. Mori, Jpn. J. Appl. Phys. 35, 6579 (1996).
5 M. Alexe, C. Harnagea, D. Hesse and U. Gösele, Appl. Phys. Lett. 75, 1793 (1999).
6 C. Harnagea, M. Alexe, J. Schilling, J. Choi, R. B. Wehrspohn, D. Hesse and U. Gösele, Appl. Phys. Lett. 83, 1827 (2003).
7 A. Stanishevsky, B. Nagaraj, J. Melngailis, R. Ramesh, L. Khriachtchev and E. McDaniel, J. Appl. Phys. 92, 3275 (2002).
8 A. Roelofs, T. Schneller, K. Szot and R. Waser, Appl. Phys. Lett. 81, 5231 (2002).
9 I. Szafraniak, C. Harnagea, R. Scholz, S. Bhattacharyya, D. Hesse and M. Alexe, Appl. Phys. Lett. 83, 2211 (2003).
10 S. Bühlmann, P. Muralt and S. V. Allmen, Appl. Phys. Lett. 84, 2614 (2004).
11 M. Shimizu, H. Fujisawa, H. Niu and K. Honda, J. Cryst. Growth 237-239, 448 (2002).
12 H. Nonomura, H. Fujisawa, M. Shimizu, H. Niu and K. Honda, Jpn. J. Appl. Phys. 42, 5918 (2003).
13 H. Fujisawa, M. Okaniwa, H. Nonomura, M. Shimizu and H. Niu, J. Eur. Ceram. Soc. 24, 1641 (2004).
14 H. Nonomura, H. Fujisawa, M. Shimizu, H. Niu and K. Honda, Jpn. J. Appl. Phys. 43, 6542 (2004).
15 H. Nonomura, M. Nagata, H. Fujisawa, M. Shimizu, H. Niu and K. Honda, Appl. Phys. Lett. (submitted) (2004).
16 J. Tersoff and R. M. Tromp: Phys. Rev. Lett. 70 (1993) 2782.

(Received December 23, 2004; Accepted January 31, 2005)